Spectral identification in the attogram regime through laser-induced emission of single optically-trapped nanoparticles in air

Pablo Purohit, Francisco J. Fortes and J. Javier Laserna*

Departamento de Química Analítica, Universidad de Málaga, Campus de Teatinos S/N,29071, Malaga (Spain) Email: laserna@uma.es

ABSTRACT: Current trends in nanoengineering are bringing along new structures of diverse chemical compositions that need to be meticulously defined in order to ensure their correct operation. Few methods can provide the sensitivity required to carry out measurements on individual nano objects without tedious sample pre-treatment or data analysis. In the present study, we introduce a pathway for the elemental identification of single nanoparticles (NPs) that avoids suspension in liquid media by means of optical trapping and laser-induced plasma spectroscopy. We demonstrate spectroscopic detection and identification of individual 25 (± 3.7) to 70 (± 10.5) nm in diameter Cu NPs stably trapped in air featuring masses down to 73 ± 35 attograms. We found an increase in the absolute number of photons produced as size of the particles decreased; pointing towards a more efficient excitation of ensembles of only ca. 7 x 10^5 Cu atoms in the onset plasma.

Keywords: Attogram identification • Copper • Laser spectroscopy • Optical trapping in air • Single nanoparticle analysis

Nanodevices are steadily making their way into an increasing number of applications over a wide range of fields such as electronics[1] or biomedicine[2], which take advantage of unique features derived from their structure. The individual characterization of these materials demands a great degree of sensitivity. Suitable techniques ranging from spectroscopy[3] to mass spectrometry (MS)[4] or electrochemistry[5] have already been proposed. The mentioned methodologies are not exempt of drawbacks, mostly related to difficult isolation of the NPs and the discrimination of the events produced by an individual particle. Other frequent constraints are the need of transferring samples to stabilized liquid media where other chemical species can potentially lead to data alteration or the low number of elements that can be identified simultaneously, caused by instrumental restrictions as in single particle-MS.[6] Seeking to avoid sample pre-treatment while offering extreme sensitivity and multi-component detection for single NP analysis, we present a method based in the combination of optical trapping[7] (OT) and laser-induced breakdown spectroscopy[8] (LIBS). In this approach, sample nanopowder deposited on a support and placed inside a cuvette is catapulted into solid aerosol form by air plasma shockwaves. A single particle is secluded in the optical trap set by a CW laser as the aerosol spreads through the cuvette. Excitation is performed by a single laser shot and full optical emission spectrum from the particle plasma is collected. We set our focus in Cu NPs analysis for the current work. The presence and relevance of Cu in nanotools is increasing[9] as a substitute for other noble metals (Au and Ag) due to its similar properties, wider availability and the progressive overcome of negative features, e.g., low resistance to oxidation. OT-LIBS was previously used for analysis of single particles such as graphite, Ni or Al_2O_3 with diameters down to 100 nm[10]. Herein, we report the first application of OT-LIBS to particles below the 100 nm size threshold. The probing of such NPs, with masses down to the attogram regime, paves the way to set new extreme limits of detection in optical spectroscopy.

The custom-built experimental setup is shown in Figure 1. In addition to the OT and LIBS lines, the instrument included a visualization line consisting on a CMOS camera for particle tracking and an imaging line with an iCCD camera used to align the system to its origin of coordinates, for plasma imaging and to monitor the contactless NP manipulation. Position of the particle was modified as needed along the z axis until placed at (0,0,0), where spectral identification was conducted. Qualitative portions of Cu nanospheres of average sizes 25, 50 and 70 nm were used for the experiments and could be recovered and reused after measuring. Physical characteristics of the samples are given in Table S1.

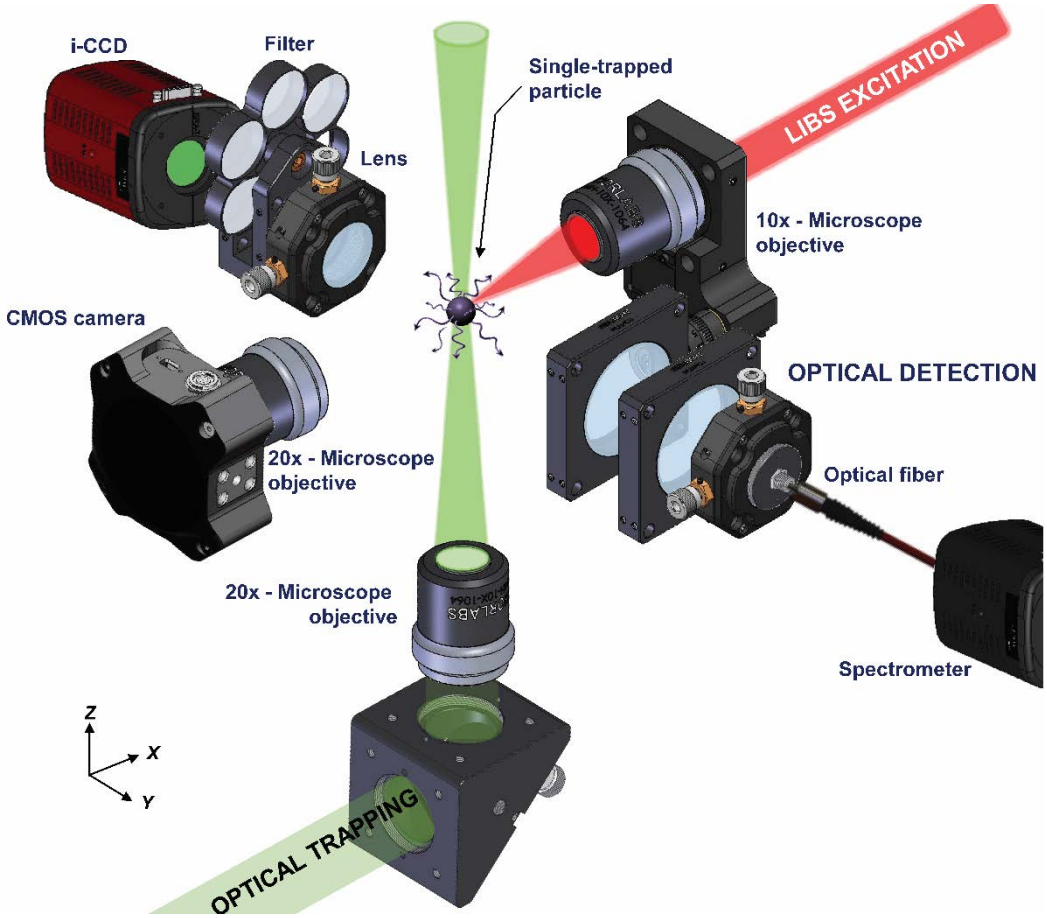

Figure 1. Experimental setup featuring the multiple lines of the instrument with main components labelled. Optical trapping was performed using a 532 nm Nd:YAG CW laser and a pulsed Nd:YAG at 1064 nm was used for LIBS analysis.

We utilized a long working distance (WD) and, consequently, low numeric aperture (NA) microscope objective to focus the trapping beam, delivering 140 mW at the sample plane. The use of such objective allowed trapping at several mm from the sample support and particle manipulation over a large length (~ 5 mm for the higher diameter particles) at the cost of reduced radiation pressure at focus. This was crucial to avoid interference of material re-deposited at the support in the measurements. Besides, locating the optical trap far from high particle density regions reduced the number of aerosol-isolated NP collisions, facilitating trapping. Low forces could potentially affect LIBS sampling rate due to the particle position not being steady enough to assure interaction with the excitation laser. To quantitatively evaluate the optical forces acting upon trapped particles, the trap was calibrated for each sample diameter by tracking their Brownian motion. From calibration (see Supporting Information), stiffness of the trap was accessible via its characteristic spring constant k, which accounts for displacements of the particle from its

equilibrium position. Figure 2A shows the values of the radial spring constant (k_y) and the axial spring constant (k_z) for each sample. Trapping strength increased with particle size, as reported for optically trapped Au NPs in air.[11] From the equilibrium position (0,0,0), trapped particles could randomly travel distances of ca. ±35 µm along the z axis within a few minutes as detailed in Figure 2B. These observed displacements were below the Brownian diffusion radius (Figure S1) estimated by trajectory simulation in air when no optical trap is set (Supporting Information). Thus, we can confirm that trapping was stable enough to overcome diffusion and confine the particle within a controlled space. Although large, random fluctuations posed no major inconvenient during characterization. As exemplified by Figure 2C (I) and (II) particles could be manipulated along wide gaps in order to be placed at (0,0,0) position and guarantee its interception by the LIBS laser, which was focused to a spot of 100 µm. Moreover, as excitation source[10b,12], covered the entire NP, resulting in 100% sampling efficiency.

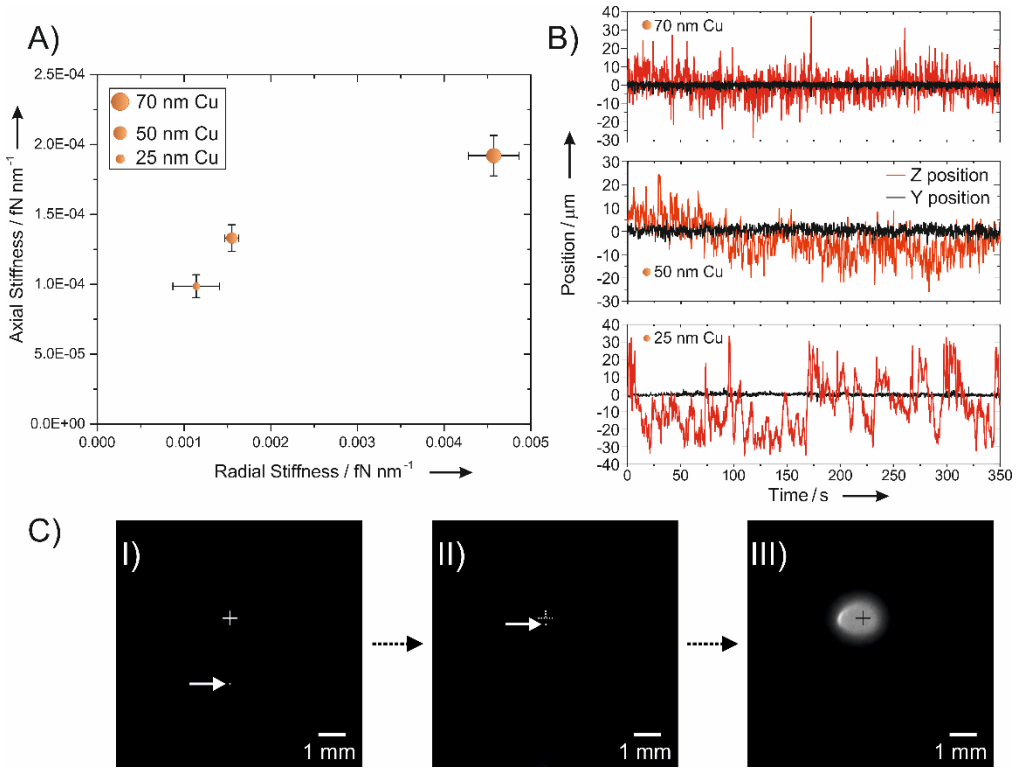

Figure 2. A) Radial and axial stiffness for each particle size. B) Trajectory of a 70 nm, 50 nm and 25 nm particle trapped at (0,0,0) due to Brownian motion. C) (I, II) Contactless manipulation of a trapped 70 nm Cu particle up to (0,0,0) position. The whitearrows highlight the particle position while crosses mark the origin of coordinates. (III) Morphology a plasma ignited on the particle (2 ns after the onset); air is ionized alongside the particle, hence the size and appearance of the plasma.

Metallic Cu is known to possess localized surface plasmon resonance (LSPR), usually featuring extinction maxima at wavelengths (λ) ca. 600 nm.[13] Previous reports indicate that trapping with λ close to or below plasmon resonance is unlikely.[14] Nevertheless, we successfully isolated each Cu sample for times spanning from minutes to beyond an hour (50 and 70 nm particles) despite using a trapping λ below Cu LSPR, i.e. 532 nm laser radiation. Further discussion on the physics involved in the process and results of studies conducted on 90 nm Ag and Au NPs are provided in the Supporting Information. It should be mentioned that, at sub-fN nm^{-1} optical forces, the attraction exerted by gravity upon samples (F_g= 7.19 e^{-4}, 5.75 e^{-3} and 1.57 e^{-2} fN for 25, 50 and 70 nm respectively) is in the same order of optical forces in the Z axis. This force may contribute to trapping by counteracting the repulsive light momentum force.

As the waist of the described optical trap was 5.9 μm, several particles could get trapped simultaneously at (0,0,0). This scenario presented a hindrance for single NP inspection since particles were separated by distances below the spatial resolution of the LIBS analysis and were consequently consumed as a cluster by the laser-induced plasma. LIBS emission signal depends directly on the sample mass incorporated into the plasma. To uncover whether a single NP or a cluster were actually trapped on the system, a sorting method was used. In this approach, events in data series exhibiting lower intensities of the Cu (I) line at 324.75 nm were considered to point out single particle excitation. Figure 3 illustrates the method applied to a 70 nm Cu data set. First, we calculated the net intensity of every event and discarded those corresponding to very large signals, attributed to clusters. Also, signals with a signal-to-noise ratio (SNR) below 3 were removed as we observed that they corresponded to particles trapped away from the (0,0,0) position by a length from 2 to 3 times the laser spot size. Particles located beyond provided no signal at all. A gap separating low I events became clear as seen in Figure 3B. Mean I (μ_{events}) of the circled events in Figure 3C was calculated to set the upper limit of single particle detection to μ_{events} +3s_{events} (the standard deviation of μ_{events}). The lower limit was set as three times the standard variation of the encircled events' background. This range covered signal fluctuation sources such as shot-to-shot energy variation and size dispersion of the sample. No events other than those first assumed as single NPs fell within the limits as shown in the same panel. The sorting of 50 nm and 25 nm Cu particles can be seen in Figure S6.

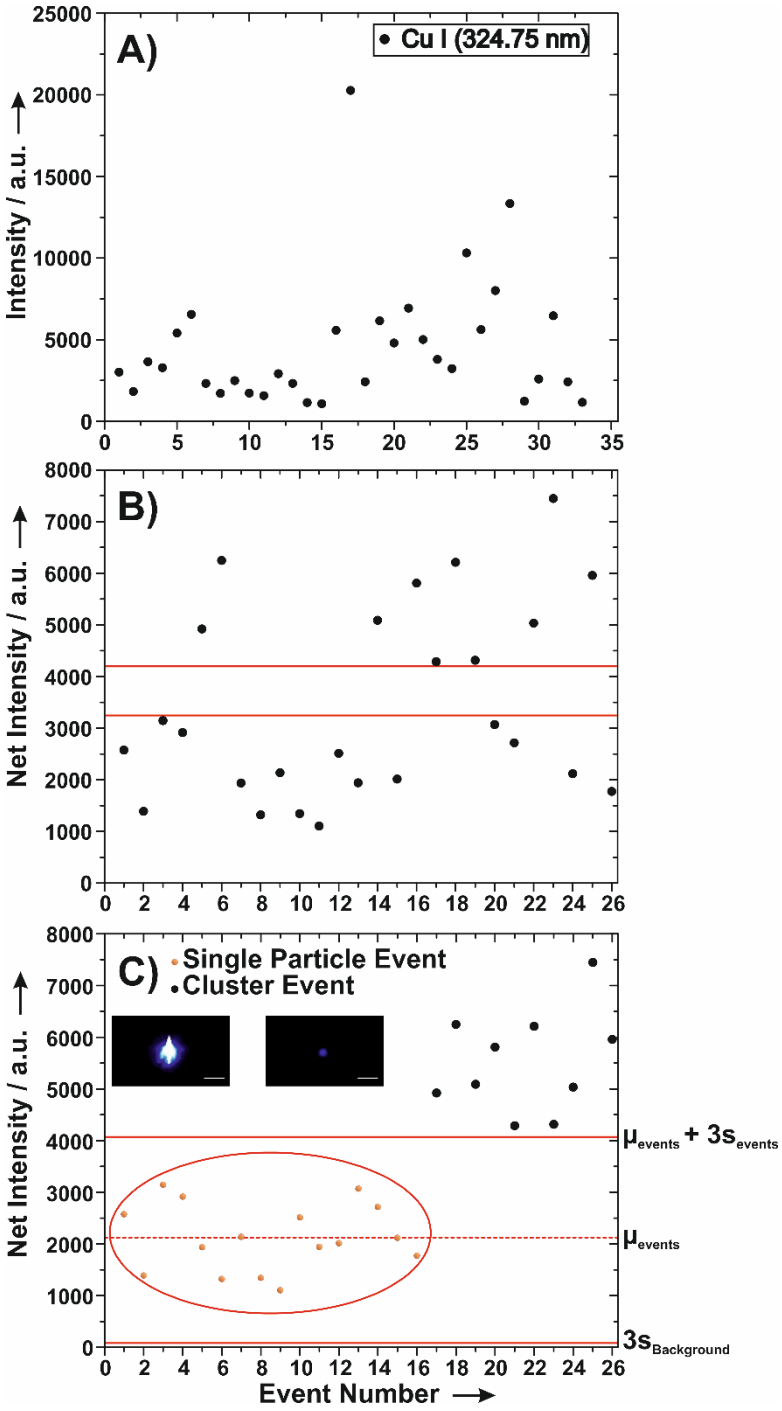

Figure 3. Sorting of a 70 nm particles data set. A) Raw data set. B) Net intensity of surviving events after exclusion of large clusters and signals with SNR below 3. Red lines indicate the gap separating high and low net intensity regions C) Attribution of single particle events according to the criteria described in the main text. Events were gathered for clarity. Dashed horizontal line marks the mean intensity (μ) of the points within the straight horizontal lines. Those lines limit the single-particle intensity window. The inset in C) shows scattering images of two trapped entities. Although scattering intensity and size of the image can be used to identify large clusters (left), single particles can be discriminated from smaller clusters only through LIBS (right). Scale bars = 200 μm.

Figure 4 shows the average intensity for each particle diameter after using the classification scheme. As expected, Cu signal increased proportionally to particle size. The signal-to-noise ratio (SNR) for the classified data was calculated from Equation (1):

$$SNR = \frac{\mu_{Average\ Net\ I}}{3s_{Background}} \quad (1)$$

SNR values were 26, 17 and 6 for 70, 50 and 25 nm Cu respectively (see Table S2 for details). Thus, we can state that OT-LIBS is able to detect and identify Cu NPs of 73 attogram mass. After linearly fitting net intensity versus particle mass, limit of detection (LOD) for Cu was estimated from Equation (2):

$$LOD = y_b + 3s_b \quad (2)$$

where y_b is the average intensity of a blank for each diameter and s_b is their average standard deviation. LOD = 58.9 ± 1.8 ag, the mass of a 23 nm NP, was established.

The observed linearity suggests that the particles were completely atomized in the plasma. Still, this fact is not equivalent to excitation of every resulting atom. To quantify the excitation efficiency we backtracked the collected light's path from the detector to the plasma which originated it.[10a] The number of photons required to spawn a single intensity unit in the detector at the monitored wavelength (324.75 nm) was estimated according to Equation (3):

$$S = \frac{\omega_d}{Q_E \psi} \quad (3)$$

where S is the sensitivity of the detector, ω_d is the pixel well depth, Q_E is the quantum efficiency and ψ is the spectrometer's 16-bit AD converter. The total number of detected photons was then calculated for a given net intensity. Losses due to traversed optical surfaces were then added as illustrated in Figure S7. Following this analysis, we found a higher degree of excitation for smaller particles. Figure 4 shows the photon yield per sample gram associated to each inspected sample size. NPs of 25 nm diameter yielded one order of magnitude more photons (1.26×10^{23} photons g^{-1}) than the 70 nm ones (1.34×10^{22} photons g^{-1}) despite having a mass two orders of magnitude lower.

Results can be discussed on the basis of the energy required for complete particle dissociation. Samples were irradiated using the same pulse energy (260 mJ), mostly consumed to spark and develop the air-particle plasma. Air plasma acted as the main excitation source over direct pulse-NP interaction[12] hence, the dissociation and excitation

processes were governed by heat transmission from the plasma to the particle and by mass transfer from the particle to the plasma. The amount of energy to be supplied by the plasma in order to fully overcome the atomic bonding is higher for larger particles. Therefore, for plasmas of identical characteristics, a larger part of excitation energy was available for promotion to emissive states of dissociated Cu atoms from 25 nm NPs, hence the higher photon yield. When excitation energy was raised to the maximum output given by the LIBS laser (280 mJ), signal increases were observed for each particle size. Thus corroborating the proposed idea under our experimental conditions (Table S3). The large excitation efficiency of small particles is a key element in the attogram sensitivity of OT-LIBS.

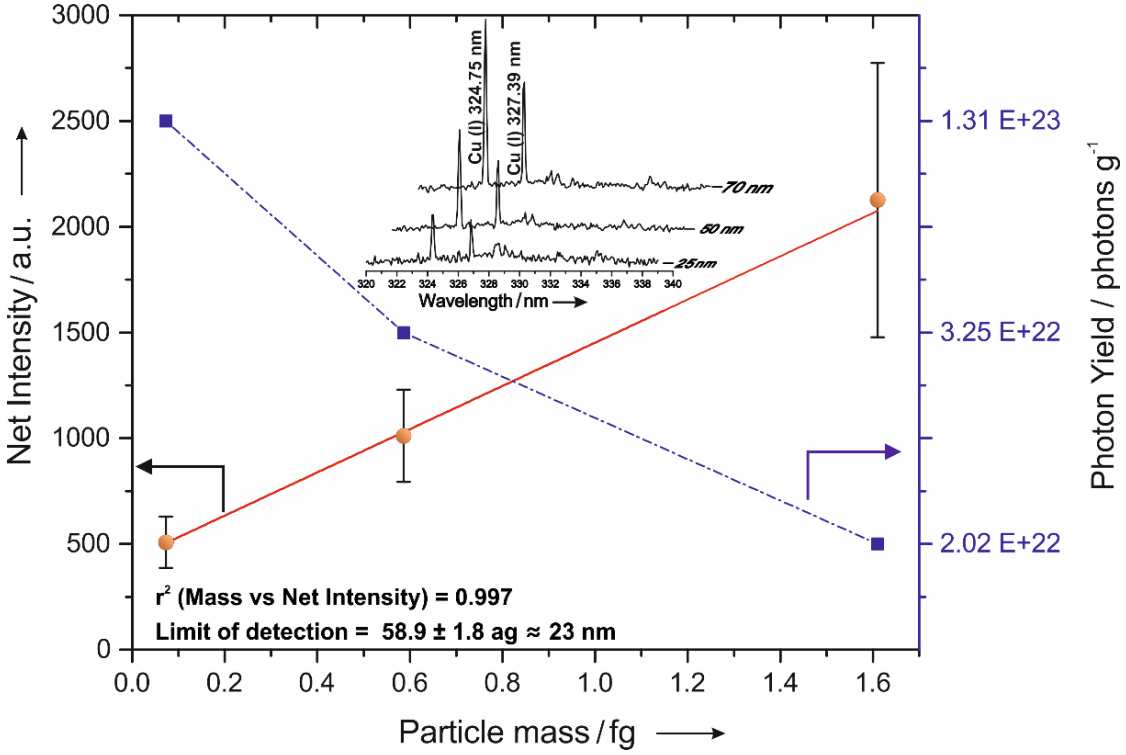

Figure 4. Correlation between each particle's net emission intensity and its mass (straight line) and absolute production of photons per mass unit for each diameter particle (dashed line).Inset shows the average spectra for different size Cu NPs. Spectra were shifted for clarity.

We have presented a size-sensitive tool combining optical trapping and laser-induced breakdown spectroscopy able to explore full chemical composition of single NPs isolated within an optical trap in air with masses in the attogram regime. The technique features an unprecedented LOD in optical emission spectroscopy of 58.9 ± 1.8 ag. This extreme sensitivity is due to increased excitation efficiency of smaller particles in laser-induced plasmas as described here. The technique could support new analytic methods over different scientific fields for identification and assessment of the presence of trace

elements in complex structures including composite NPs, nanosensors, nanocarriers or even living cells.

Acknowledgements

Research funded by the Spanish Ministerio de Economia y Competitividad under Project CTQ2014-56058P. P. Purohit gratefully acknowledges the concession of a FPI grant associated to the same project.

References

[1] a) J. N. Freitas, A. S. Gonçalves, A. F. Nogueira, Nanoscale 2014, 6, 6371–97; b) A. Kamyshny, S. Magdassi, Small 2014, 10, 3515–3535.

[2] G. De Crozals, R. Bonnet, C. Farre, C. Chaix, Nano Today 2016, 11, 435–463.

[3] A. Crut, P. Maioli, N. Del Fatti, F. Vallée, Chem. Soc. Rev. 2014, 43, 3921–3956.

[4] M. D. Montaño, J. W. Olesik, A. G. Barber, K. Challis, J. F. Ranville, Anal. Bioanal. Chem. 2016, 408, 5053–5074.

[5] a) L. R. Holt, B. J. Plowman, N. P. Young, K. Tschulik, R. G. Compton, Angew. Chem. Int. Ed. 2016, 55, 397–400; Angew. Chem. 2016, 128, 405–408; b) S. Nizamov, O. Kasian, V. M. Mirsky, Angew. Chem. Int. Ed. 2016, 55, 7247–7251; Angew. Chem. 2016, 128, 7363–7367.

[6] M. D. Montaño, H. R. Badiei, S. Bazargan, J. F. Ranville, Environ. Sci. Nano 2014, 1, 338.

[7] O. M. Maragò, P. H. Jones, P. G. Gucciardi, G. Volpe, A. C. Ferrari, Nat. Nanotechnol. 2013, 8, 807–19.

[8] F. J. Fortes, J. Moros, P. Lucena, L. M. Cabalín, J. J. Laserna, Anal. Chem. 2013, 85, 640–669.

[9] a) S. Magdassi, M. Grouchko, A. Kamyshny, Materials. 2010, 3, 4626–4638; b) C. Wang, L. Ling, Y. Yao, Q. Song, Nano Res. 2015, 8, 1975–1986; c) J. Sun, T. Hu, X. Xu, L. Wang, X. Yang, Nanoscale 2016, 8, 16846–16850.

[10] F. J. Fortes, A. Fernández-Bravo, J. J. Laserna, Spectrochim. Acta - Part B At. Spectrosc. 2014, 100, 78–85; b) P.Purohit, F.J. Fortes, J. J. Laserna, Spectrochim. Acta - Part B At. Spectrosc. 2017, 130, 75–81.

[11] L. Jauffred, S. M. R. Taheri, R. Schmitt, H. Linke, L. B. Oddershede, Nano Lett. 2015, 15, 4713–4719.

[12] a) D. W. Hahn, N. Omenetto, Appl. Spectrosc. 2010, 64, 335A–366A; b) V. Hohreiter, D. W. Hahn, Anal. Chem. 2006, 78, 1509–14.

[13] a) G. H. Chan, J. Zhao, E. M. Hicks, G. C. Schatz, R. P. Van Duyne, Nano Lett. 2007, 7, 1947–1952; b) M. D. Susman, Y. Feldman, A. Vaskevich, I. Rubinstein, Chem. Mater. 2012, 24, 2501–2508.

[14] a) J. R. Arias-González, M. Nieto-Vesperinas, J. Opt. Soc. Am. A 2003, 20, 1201; b) J. Prikulis, F. Svedberg, M. Käll, J. Enger, K. Ramser, M. Goksör, D. Hanstorp, Nano Lett. 2004, 4, 115–118.